

# Theoretical approach to Resonant Inelastic X-ray Scattering in iron-based superconductors at the energy scale of the superconducting gap

Pasquale Marra,<sup>1</sup> Jeroen van den Brink,<sup>2,3</sup> and Steffen Sykora<sup>2</sup>

<sup>1</sup>*CNR-SPIN, I-84084 Fisciano (Salerno), Italy*

<sup>2</sup>*Institute for Theoretical Solid State Physics, IFW Dresden, D-01069 Dresden, Germany*

<sup>3</sup>*Department of Physics, TU Dresden, D-01062 Dresden, Germany*

(Dated: May 23, 2014)

We develop a phenomenological theory to predict the characteristic features of the momentum-dependent scattering amplitude in resonant inelastic x-ray scattering (RIXS) for the case of the iron-based superconductors. Taking into account all relevant orbital states as well as their specific content along the Fermi surface we evaluate for the compounds LaOFeAs and LiFeAs the dynamical structure factors of charge and spin based on tight-binding models, which are fully consistent with recent angle-resolved photoemission spectroscopy (ARPES) data. While the orbital content strongly modifies the momentum dependence of RIXS intensities, we find considerable enhancement of the intensity of sign reversing excitations in the spin structure factor. Moreover, a characteristic intensity redistribution between spin and charge transfer excitations is found in case of antisymmetric momentum dependence of the superconducting order parameter. Consequently, our results show that RIXS spectra can discriminate between  $s_{\pm}$  and  $s_{++}$  wave gap functions in the singlet pairing case. In addition, a possible triplet pairing based on chiral  $p$  wave gap function affects the intensity at small momenta and can be distinguished from singlet pairing.

PACS numbers: 78.70.Ck, 74.70.Xa, 74.20.Rp

## I. INTRODUCTION

One of the first steps to study the pairing mechanism in unconventional superconductors is the characterization of the superconducting state with respect to its orbital symmetry and phase. Whereas in conventional superconductors the superconductivity is based on an effective coupling mediated by lattice distortions, in the case of high  $T_c$  superconductors we expect electronic correlations to be responsible of the pairing<sup>1</sup>, leading to characteristic variations of the energy gap along the Fermi surface<sup>2-4</sup>. Thus, the corresponding order parameter, which describes the momentum dependent coupling strength between the electrons within one Cooper pair, shows a variation in momentum space indicating strong correlations taking place over rather short distances. Moreover, while the SC gap function of conventional superconductors has the same phase throughout momentum space ( $s$  wave symmetry), that of correlation mediated superconductors is expected to exhibit a sign reversal between those Fermi momenta connected by characteristic wave vector  $\mathbf{Q}_{AF}$  of spin fluctuations<sup>5</sup>. In  $d$  wave superconductors, the nodal planes of the order parameter intersect with the Fermi surface, leading to gapless quasiparticle (QP) excitations that can be detected thermodynamically and by low energy probes. However, a sign reversal of the SC order parameter can also occur (without the presence of nodal excitations) between disconnected hole and electron pockets resulting in an  $s_{\pm}$  symmetry<sup>6,7</sup>. This scenario is expected in most of the iron-based superconductors, and there the relative sign change of SC gap must be determined by phase-sensitive experiments such as Josephson junctions experiments<sup>8</sup>, composite SC loops<sup>9</sup>, and scanning tunneling microscopy

(STM)<sup>10-14</sup>. Of particular interest in this context is the material LiFeAs since experiments have proven an absence of nesting<sup>15,16</sup> and theoretical works yield contradictory results; i.e., both different configurations of  $s$ -wave singlet<sup>17-19</sup> as well as  $p$ -wave triplet pairing have been suggested<sup>20</sup>.

In general, the correct interpretation of phase-sensitive experiments requires detailed information about the low energy properties of the material, like for example the normal state band structure, correlations, or the type of impurity scattering. Moreover, in pnictide superconductors it is well known that the orbital physics play a very important role, in particular, the variation of orbit content along the Fermi surface. In most cases it is the insufficient knowledge about these properties which prevents the characterization of the superconducting state directly from measured spectra. Time reversal symmetry breaking of the system by use of an external magnetic field, which is known to enhance the QP excitations with preserved sign of SC order parameter<sup>21</sup>, is one possible way to overcome these problems. Recently, this method has been applied to the iron-based superconductor Fe(Se,Te)<sup>22</sup> and results of this study have been considered as evidence for  $s_{\pm}$  pairing in this material. However, this interpretation raised a number of comments<sup>23</sup>, as for example the field effect in iron-based superconductors is expected to differ significantly from the one observed in cuprates. Moreover, in this material, the Zeeman splitting is a large fraction of the superconducting gap size, generating new components to the field induced scattering<sup>24</sup>.

Very recently, we have shown that resonant inelastic x-ray scattering (RIXS) appears as an additional experimental method which is sensitive to phase and orbital

symmetry of SC order parameters<sup>25</sup>. In the past decade, this spectroscopic technique has established as an experimental probe of elementary spin<sup>26</sup>, orbital<sup>27</sup>, and lattice excitations<sup>28</sup>. In particular, the direct RIXS process<sup>29</sup> allows spin flip excitations if the spin of conduction electrons has components parallel to the  $x^2 - y^2$  orbital<sup>30</sup>. This fact offers the possibility to probe the momentum-dependent charge and spin dynamical structure factors  $\chi^{c,s}(\mathbf{q}, \omega)$  of the bulk system<sup>25</sup> where the corresponding form factors can be adjusted by the specific geometry of the experiment and the polarization of the incoming photon beam. The well known property of the spin-spin correlation function  $\chi^s(\mathbf{q}, \omega)$  to enhance sign reversing scattering, leading for example to the famous 41 meV resonant mode in cuprates, would place the RIXS experiment (applied to the iron-based superconductors) on the same footing as the QP interference in magnetic field – with the additional advantage that the interpretation of spectroscopic features does not rely on the modeling of impurity scattering. How effective are these arguments in the presence of a strong variation of orbital content along the Fermi surface and to what extent we can expect signatures of the superconducting order parameter phase in the spectra?

In the following will will investigate the RIXS response of iron-based superconductors at an energy scale that corresponds roughly to the superconducting gap. Previously the Fe  $L_3$ -edge RIXS response of such systems at higher loss-energies, corresponding to the magnetic and orbital excitations has been studied theoretically<sup>31</sup>, establishing that magnon excitations, predominantly composed of a single orbital component, can be seen in experiments, with a spectral weight that is smaller than spin-flipped interorbital excitations at still higher energies. This theoretical work stimulated a subsequent experimental study<sup>32</sup>, which not only confirmed the presence of the magnon excitations in an energy range up to an energy of 200 meV in magnetically ordered iron-pnictides<sup>33</sup>, but also revealed the persistence of magnon-like modes in this energy range as the material is doped and becomes superconducting. This connects Fe pnictides to cuprates, for which, in spite of fundamental electronic structure differences, similar paramagnons are present<sup>34–36</sup>. It also motivates the question whether and how RIXS can pick up the signatures of the superconducting gap in the iron-based superconductors. Such excitations are on an energy-scale that is about an order of magnitude smaller than the 200 meV of the magnon dispersion, so that measuring them will be a challenge for RIXS experiments in the years to come – here we will set the stage for such experiments from a theoretical perspective.

Motivated by the above considerations this paper develops a phenomenological approach to the momentum and energy dependent RIXS spectrum in iron-based superconductors, taking into account the relevant orbitals of the iron ions and their different weights along the hole and electron pockets. Using tight-binding models,

derived from angle-resolved photoemission spectroscopy (ARPES), for the band structure of two important pnictide representatives LaOFeAs and LiFeAs we calculate the dynamical structure factors of charge and spin for different scenarios of superconducting pairing. Our study shows that the orbital content along the Fermi surface leads to strong suppression of spectral intensity for excitations combining orthogonal orbital states. Despite this strong effect we find that a sign change between hole and electron pocket ( $s_{\pm}$  wave) can still be detected by RIXS. In particular we show that sign reversing excitations appear as strong intensity peak in the spin sensitive spectrum at the characteristic wave vector  $\mathbf{Q}_{AF}$  of spin fluctuations. Moreover, based on these considerations, we present a way how RIXS could detect the presence of possible triplet pairing.

The paper is organized as follows. In Section II, we develop the theory to calculate superconducting QP excitations in systems with more than one relevant orbitals close to the Fermi level. A comparison of results for different types of modeling based on the orbital model and the corresponding energy band model, where the orbital variation is neglected, is shown in Section III A. We then apply our theory to the compound LiFeAs and present in Section III B calculated RIXS spectra where we assume different types of superconducting pairing ( $s_{\pm}$ ,  $s_{++}$ ,  $p$  wave). We conclude in Section IV.

## II. RIXS CROSS SECTION IN IRON-BASED SUPERCONDUCTORS

In a *direct* RIXS process at any transition-metal (TM) ion  $L$  edge, the incoming photon excites a core shell  $2p$  electron into the  $3d$  shell, which consequently decays into an outgoing photon and a charge, spin, or orbital excitation in the electronic system<sup>29</sup>. In the case of iron-based superconductors considered in this work, we have to take into account more than one relevant orbital states of the  $3d$  shell. Note that this multi-orbital structure leads to the characteristic disconnected Fermi surface sheets dominating the low energy properties in these materials. Using the fast collision approximation<sup>29,30,37</sup> the RIXS cross section can be decomposed into a combination of the charge and the spin dynamical structure factor (DSF) of  $d$  electrons as<sup>25,31,37,38</sup>

$$I_{\mathbf{e}}(\mathbf{q}, \omega) = \sum_{\alpha} |W_{\alpha\mathbf{e}}^c|^2 \chi_{\alpha}^c(\mathbf{q}, \omega) + |\mathbf{W}_{\alpha\mathbf{e}}^s|^2 \chi_{\alpha}^s(\mathbf{q}, \omega), \quad (1)$$

where

$$\chi_{\alpha}^c(\mathbf{q}, \omega) = \sum_f |\langle f | \rho_{\alpha\mathbf{q}} | i \rangle|^2 \delta(\hbar\omega + E_i - E_f), \quad (2)$$

$$\chi_{\alpha}^s(\mathbf{q}, \omega) = \sum_f |\langle f | S_{\alpha\mathbf{q}}^z | i \rangle|^2 \delta(\hbar\omega + E_i - E_f), \quad (3)$$

are the charge and spin DSF corresponding to the orbital  $\alpha$ . Note that the spin DSF is assumed to have the

same momentum and energy dependence for any direction of the spin<sup>39</sup>. The states  $|i\rangle$  ( $|f\rangle$ ) denote the initial (final) state of RIXS process with energy  $E_i$  ( $E_f$ ) where  $\hbar\omega$  ( $\mathbf{q}$ ) is the transferred photon energy (momentum). Here, the density and the spin of  $d$  electrons  $\rho_{\alpha\mathbf{q}} = \sum_{\mathbf{k}\tau} d_{\alpha\tau\mathbf{k}+\mathbf{q}}^\dagger d_{\alpha\tau\mathbf{k}}$  and  $S_{\alpha\mathbf{q}}^z = \sum_{\mathbf{k}\tau\tau'} d_{\alpha\tau\mathbf{k}+\mathbf{q}}^\dagger \sigma_{\tau\tau'}^z d_{\alpha\tau'\mathbf{k}}$  are defined in terms of the orbital operator  $d_{\alpha\tau\mathbf{k}}^\dagger$  ( $d_{\alpha\tau\mathbf{k}}$ ), which creates (annihilates) an electron in the orbital  $\alpha$  with spin  $\tau$  and momentum  $\mathbf{k}$ . The RIXS form factors  $W_{\alpha\mathbf{e}}^c$  and  $\mathbf{W}_{\alpha\mathbf{e}}^s$  in Eq. (1) depend on the TM ion, the orbital symmetry of the system, the specific geometry of the experiment, and on the polarization  $\mathbf{e}$  of the incoming and outgoing x-ray beams<sup>30,37,38</sup>. Thus, these parameters can be adjusted in the RIXS experiment, and therefore, under construction of particular experimental setups, the cross section will be solely determined either by the charge or by the spin DSF. As it has been shown in Ref. 25, this property can be used to reveal the character of the pairing mechanism in SC materials. Motivated by this idea, we study in this paper the charge and spin DSF for iron-based superconductors using accepted band structure models, and comparing different pairing mechanisms and order parameter symmetries.

The usual way to describe phenomenologically the unconventional SC state in many-particle systems is based on a generalized multi-band mean-field Hamiltonian of the form<sup>21,40</sup>

$$\mathcal{H} = \sum_{i\tau\mathbf{k}} \varepsilon_{i\mathbf{k}} c_{i\tau\mathbf{k}}^\dagger c_{i\tau\mathbf{k}} - \frac{1}{2} \sum_{i\tau\mathbf{k}} \xi_\tau \left( \Delta_{\mathbf{k}} c_{i\tau\mathbf{k}}^\dagger c_{i-\tau-\mathbf{k}}^\dagger + \Delta_{\mathbf{k}}^* c_{i-\tau-\mathbf{k}} c_{i\tau\mathbf{k}} \right), \quad (4)$$

where the operator  $c_{i\tau\mathbf{k}}^\dagger$  ( $c_{i\tau\mathbf{k}}$ ) creates (annihilates) an electron with spin  $\tau$  in the energy band  $i$ , which is described by the bare electron dispersion  $\varepsilon_{i\mathbf{k}}$ , and with  $\Delta_{\mathbf{k}}$  the momentum-dependent SC order parameter. The second term in Eq. (4) is responsible for the superconducting state, with the pairing character determined by  $\xi_\tau$ . The case of  $\xi_\tau = \pm 1$  for up and down spin describes the spin-singlet pairing, whereas the case  $\xi_\tau = 1$  for both spin directions leads to a special type of spin-triplet state. In general, the triplet pairing term is given by  $-\frac{1}{2} \Delta_{\mathbf{k}\tau\tau'} c_{i\tau\mathbf{k}}^\dagger c_{i\tau'\mathbf{k}}^\dagger + \text{h.c.}$ , with a multi-component SC order parameter of the form  $\Delta_{\mathbf{k}\tau\tau'} = i[\mathbf{d}(\mathbf{k}) \cdot \boldsymbol{\sigma}] \sigma_y$  (see, e.g., Ref. 40). However, in this paper we consider only the simplest case  $d_x(\mathbf{k}) = d_y(\mathbf{k}) = 0$  and  $d_z(\mathbf{k}) = \Delta_{\mathbf{k}}$ , and therefore the gap function simplifies to  $\Delta_{\mathbf{k}\uparrow\uparrow} = \Delta_{\mathbf{k}\downarrow\downarrow} = 0$  and  $\Delta_{\mathbf{k}\uparrow\downarrow} = \Delta_{\mathbf{k}\downarrow\uparrow} = \Delta_{\mathbf{k}}$ .

To investigate the RIXS cross section given by Eq. (1) we calculate the DSF  $\chi_\alpha^{c,s}(\mathbf{q}, \omega)$  on the basis of the model Hamiltonian (4) separately for each of the relevant orbitals. Using the unitary transformation

$$c_{i\tau\mathbf{k}} = \sum_{\alpha} \lambda_{i\alpha\mathbf{k}} d_{\alpha\tau\mathbf{k}}, \quad (5)$$

between orbital and energy band representation we rewrite the density and spin operators  $\rho_{\alpha\mathbf{q}}$  and  $S_{\alpha\mathbf{q}}^z$  in

Eqs. (2) and (3) in terms of the operators  $c_{i\tau\mathbf{k}}$  and  $c_{i\tau\mathbf{k}}^\dagger$  in the band representation. This step is necessary for the calculation of the matrix elements and excitation energies in Eqs. (2) and (3). Note that, in general, the Hamiltonian is not diagonal with respect to the orbital states because the different orbitals can hybridize with each other. The transformation matrix elements  $\lambda_{i\alpha\mathbf{k}}$ , which describe the orbital content of conduction bands, are obtained diagonalizing the low-energy tight-binding Hamiltonian of the system. For this purpose, we consider in this paper the tight-binding model in Ref. 41 for LaOFeAs, and a slightly modified tight-binding model based on Ref. 20 for LiFeAs (see below).

Having expressed the density and spin operators in the DSF in terms of the one-particle operators in the band representation, the next step is to diagonalize the Hamiltonian (4) by a Bogoliubov transformation  $c_{i\uparrow\mathbf{k}} = u_{i\mathbf{k}}^* \gamma_{i\uparrow\mathbf{k}} - v_{i\mathbf{k}} \gamma_{i\downarrow-\mathbf{k}}^\dagger$  and  $c_{i\downarrow\mathbf{k}} = u_{i\mathbf{k}}^* \gamma_{i\downarrow\mathbf{k}} + v_{i\mathbf{k}} \gamma_{i\uparrow-\mathbf{k}}^\dagger$ , with  $|u_{i\mathbf{k}}|^2 (|v_{i\mathbf{k}}|^2) = \frac{1}{2} (1 \pm \varepsilon_{i\mathbf{k}}/E_{i\mathbf{k}})$  and  $u_{i\mathbf{k}}^* v_{i\mathbf{k}} = \frac{1}{2} \Delta_{\mathbf{k}}/E_{i\mathbf{k}}$  for each of the different bands. This allows us to find the ground state  $|\text{BCS}\rangle$  and the excitations of the system, in terms of the SC quasiparticle (QP) operators  $\gamma_{i\tau\mathbf{k}}$  and of the QP dispersion  $E_{i\mathbf{k}} = \sqrt{\varepsilon_{i\mathbf{k}}^2 + |\Delta_{\mathbf{k}}|^2}$ . In a centrosymmetric SC at zero temperature, the excited states contributing to DSF have the form  $\gamma_{j\tau\mathbf{k}+\mathbf{q}}^\dagger \gamma_{i-\tau-\mathbf{k}}^\dagger |\text{BCS}\rangle$  with energy  $E_{i\mathbf{k}} + E_{j\mathbf{k}+\mathbf{q}}$ , and the DSF of QP excitations reads finally

$$\chi_\alpha^{c,s}(\mathbf{q}, \omega) = \sum_{ij\mathbf{k}} \delta(\hbar\omega - E_{i\mathbf{k}} - E_{j\mathbf{k}+\mathbf{q}}) \times | \lambda_{i\alpha\mathbf{k}} \lambda_{j\alpha\mathbf{k}+\mathbf{q}} |^2 \left[ 1 \pm \frac{\text{Re}(\Delta_{\mathbf{k}} \Delta_{\mathbf{k}+\mathbf{q}}^*) \mp \varepsilon_{i\mathbf{k}} \varepsilon_{j\mathbf{k}+\mathbf{q}}}{E_{i\mathbf{k}} E_{j\mathbf{k}+\mathbf{q}}} \right], \quad (6)$$

where the  $\pm$  sign is for the charge (spin) DSF<sup>42–44</sup>. This result shows that the momentum-dependent DSF of low energy QP excitations is strongly affected by the orbital content of bare electrons and the structure of the superconducting order parameter.

The character of the SC pairing, which is described by the gap function  $\Delta_{\mathbf{k}}$ , arises at energies close to the Fermi level  $\hbar\omega \approx \varepsilon_F$ . There, the main contributions to the DSF correspond to excitations close to the Fermi surface, i.e., which fulfill the condition  $\varepsilon_{i\mathbf{k}} \varepsilon_{j\mathbf{k}+\mathbf{q}} \ll |\Delta_{\mathbf{k}} \Delta_{\mathbf{k}+\mathbf{q}}|$ . Assuming a phase dependent order parameter in the form  $\Delta_{\mathbf{k}} = |\Delta_{\mathbf{k}}| e^{i\phi_{\mathbf{k}}}$ , the DSF in Eq. (6) for low-energy excitations becomes approximately

$$\chi_\alpha^{c,s}(\mathbf{q}, \omega) \approx \sum_{ij\mathbf{k}} \delta(\varepsilon_{i\mathbf{k}} \varepsilon_{j\mathbf{k}+\mathbf{q}}) \delta(\hbar\omega - |\Delta_{\mathbf{k}+\mathbf{q}}| - |\Delta_{\mathbf{k}}|) \times | \lambda_{i\alpha\mathbf{k}} \lambda_{j\alpha\mathbf{k}+\mathbf{q}} |^2 [1 \pm \cos(\phi_{\mathbf{k}} - \phi_{\mathbf{k}+\mathbf{q}})]. \quad (7)$$

Hence, in addition to the orbital dependence, this quantity is significantly influenced by the order parameter phase  $\phi_{\mathbf{k}}$  on the Fermi surface. In particular, the charge DSF is suppressed for sign reversing ( $\phi_{\mathbf{k}} - \phi_{\mathbf{k}+\mathbf{q}} = \pi$ ), whereas the spin DSF is suppressed for sign preserving excitations ( $\phi_{\mathbf{k}} - \phi_{\mathbf{k}+\mathbf{q}} = 0$ ).

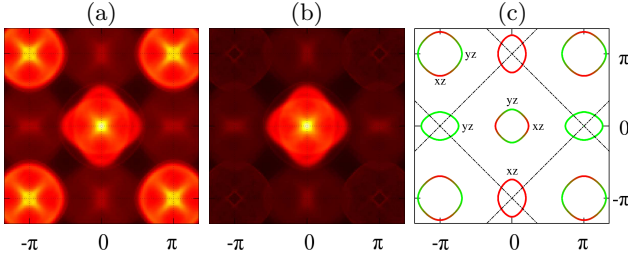


Figure 1: (color online) (a) RIXS intensities at a fixed energy loss  $\hbar\omega = 1.5\Delta_0$  as a function of the transferred momentum  $\mathbf{q}$ , for the charge DSF in LaOFeAs, assuming the  $s_{\pm}$  wave SC order parameter, calculated via Eq. (6), neglecting the orbital prefactor and assuming the bare electron dispersion of the tight-binding model in Ref. 41. (b) RIXS intensities for the same order parameter and energy loss, calculated including the effect of the orbital degrees of freedom of the electron states, summing over the contributions of the two orbitals  $\alpha = yz, zx$ . (c) Orbital content along the Fermi surface ( $yz$  and  $zx$  orbitals) as in Ref. 41. The coherence peak at  $(\pi, \pi)$ , corresponds to a nesting between the two hole pockets and between the two electron pockets respectively, which have a different orbital symmetry. For this reason, while clearly visible in (a), the coherence peak is strongly suppressed in (b), where the orbital content of the energy bands is fully taken into account.

Since the RIXS form factors  $W_{\alpha\mathbf{e}}^c$  and  $\mathbf{W}_{\alpha\mathbf{e}}^s$  in Eq. (1) can be tuned by properly choosing the experimental setup, RIXS can probe both charge and spin DSF<sup>25</sup>, which is a unique feature among other spectroscopies. A comparison of the charge and the spin DSF of QP excitations allow one to disclose not only the orbital symmetry of the ground state, but also the momentum dependence of the magnitude and of the phase of the SC order parameter and, therefore, the underlying symmetry of the pairing mechanism. In the next section we show numerical results for the two important representatives LaOFeAs and LiFeAs of the class of iron-based superconductors.

### III. NUMERICAL RESULTS

#### A. Minimal orbital model

We start by considering the effective two-band tight-binding model proposed in Ref. 41, which is regarded as a minimal model for conduction electrons in iron-based superconductors. This model contains the effective hoppings between the two orbitals  $xz$  and  $yz$  of the iron ions, within a single Fe-ion unit cell, and correctly reproduces the band structure of the compound LaOFeAs, which consists of disconnected hole-like Fermi surface sheets around  $(0, 0)$  and  $(\pi, \pi)$  and separate electron pockets of similar size around  $(0, \pm\pi)$  and  $(\pm\pi, 0)$  in the Brillouin zone [compare Fig. 1 (c)]. We assume three different symmetries for the superconducting gap, i.e.,  $s_{\pm}$  wave<sup>6</sup>,  $s_{++}$  wave<sup>46</sup>, and a spin-triplet  $p_z$  wave<sup>20</sup>,

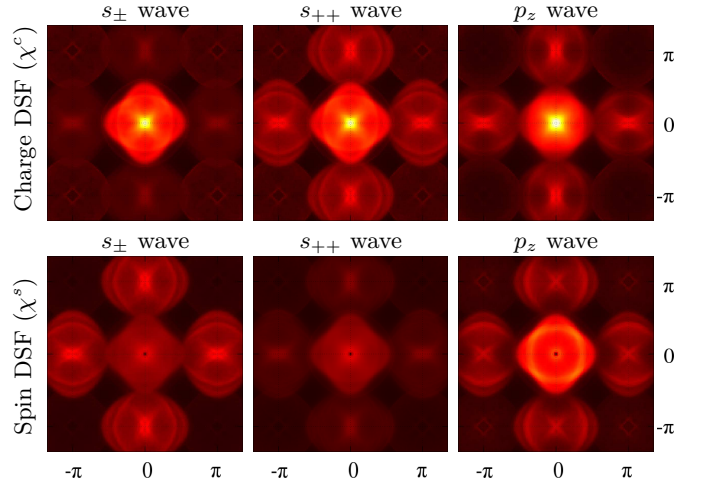


Figure 2: (color online) RIXS intensities at a fixed energy loss  $\hbar\omega = 1.5\Delta_0$  as a function of the transferred momentum  $\mathbf{q}$ , for the charge and spin DSF of QP excitations in LaOFeAs, with  $s_{\pm}$ ,  $s_{++}$ , and  $p_z$  wave SC order parameter ( $\Delta_0 = 0.1|t_1|$ , see main text), calculated using Eq. (6) and assuming the bare electron dispersion and the orbital symmetry of the tight-binding model in Ref. 41, summing over the contributions of the two orbitals  $\alpha = yz, zx$ . The coherence peak at the  $\Gamma$  point is largely dominant in the charge DSF spectra, while spectral intensities at  $\mathbf{Q}_{AF} = (\pi, 0)$  and around the  $\Gamma$  point ( $|\mathbf{q}| \approx \pi/2$ ) are sensitive to the differences in the order parameter phase along the Fermi surface. Spectral intensities at  $\mathbf{Q}_{AF}$  are strongly suppressed in the charge (spin) spectra in the  $s_{\pm}$  ( $s_{++}$ ) wave state, while intensities for  $|\mathbf{q}| \approx \pi/2$  around the  $\Gamma$  point are suppressed in the charge (spin) DSF in the  $p_z$  ( $s_{\pm}$  or  $s_{++}$ ) wave state.

where the momentum dependence is modeled respectively by  $\Delta_{\mathbf{k}}^{s_{\pm}} = \Delta_0 \cos k_x \cos k_y$ ,  $\Delta_{\mathbf{k}}^{s_{++}} = |\Delta_{\mathbf{k}}^{s_{\pm}}|$ , and  $\Delta_{\mathbf{k}}^{p_z} = \Delta_0 (\sin k_x - i \sin k_y)$ , with  $\Delta_0 = 0.1|t_1|$ , where  $t_1$  is the magnitude of the dominant near-neighbor hopping (cf. Ref. 41). For these choices of the order parameter, the gap magnitude in the spin-singlet case varies around  $\approx 0.75\Delta_0$  along the electron pockets and the inner hole pocket, and around  $\approx 0.6\Delta_0$  along the outer hole pocket, with opposite sign in the case of the  $s_{\pm}$  wave symmetry. In the spin-triplet case instead, the gap magnitude varies around  $\approx 0.65\Delta_0$  along the electron pockets and the inner hole pocket, and around  $\approx 0.83\Delta_0$  along the outer hole pocket.

At first we study the effect of the orbital variation on the spectra. In Fig. 1 is shown the charge DSF, defined in Eq. (2), at a fixed energy loss  $\hbar\omega = 1.5\Delta_0$  as a function of the transferred momentum  $\mathbf{q}$  for one particular pairing symmetry. The calculations are based on Eq. (6) using the  $s_{\pm}$  wave order parameter described above. In Fig. 1 (a) the orbital prefactors  $\lambda_{i\alpha\mathbf{k}}$  in Eq. (6) are neglected, leading to a pure band structure model. In contrast, in Fig. 1 (b) the orbital degrees of freedom have been fully taken into account. The contributions from the two orbitals  $\alpha = yz, zx$  have been summed up with equal weight since the momentum distribution of each orbital

	$t_1$	$t_2$	$t_3$	$t_4$	$t_5$	$t_6$	$t_7$	$t_8$	$t_9$	$t_{10}$	$t_{11}$	$\Delta_{xy}$
fit	0.019	0.123	0.014	-0.055	0.217	0.264	-0.137	$-t_7/2$	-0.060	-0.057	0.016	1
Ref. 20	0.020	0.120	0.020	-0.046	0.200	0.300	-0.150	$-t_7/2$	-0.060	-0.030	0.014	1

Table I: Hopping parameters for the three-band effective tight-binding model (see Ref. 20 for the definitions of the parameters and for details) compared with those fitted with the experimental Fermi surface of LiFeAs<sup>15,45</sup>. The chemical potential is  $\mu = 0.338$ , that corresponds to a filling of four electrons per site. Energy units are in electron volts.

shows qualitatively similar results. A comparison of these two panels clearly shows that the orbital content of the electron states modifies strongly the momentum dependence of RIXS spectra. In particular, the intensity peak at  $\mathbf{q} = (\pi, \pi)$  in Fig. 1 (b) is strongly suppressed, and this result is not related to the particular choice of the pairing symmetry, as confirmed by calculations based on different order parameters (not shown). This suppression originates from the fact that such transferred momentum corresponds to a nesting between branches of the Fermi surface which have a different orbital symmetry<sup>41</sup>, i.e., the two electron pockets around  $\Gamma$  and  $(\pi, \pi)$  and the two hole pockets around  $(\pi, 0)$  and  $(0, \pi)$  respectively, as shown in Fig. 1 (c). Thence, orbital degrees of freedom cannot be neglected when considering QP spectra in iron-based SC.

Furthermore, to highlight the sensitivity of DSF spectra to the order parameter phase, we show in Fig. 2 the charge and spin DSF at a fixed energy loss  $\hbar\omega = 1.5\Delta_0$  as a function of the transferred momentum  $\mathbf{q}$ , for the three choices of the order parameter defined above. As one can see, low energy excitations which are sign reversing, (opposite phase of the order parameter), suppress the charge component of the DSF, whereas sign preserving excitations (same phase of the order parameter) suppress the spin component in the low energy QP spectra. For this reason, spectral intensities at  $\mathbf{Q}_{AF} = (\pi, 0)$  in Fig. 2 are suppressed in the charge and in the spin DSF respectively in  $s_{\pm}$  wave and in the  $s_{++}$  wave SC states. Such transferred momentum corresponds to the ordering vector of the antiferromagnetic phase, and is in fact a nesting vector between the hole pockets and the electron pockets in the Brillouin zone, which have an opposite sign or the same sign of the order parameter alternatively in the  $s_{\pm}$  wave and in the  $s_{++}$  wave states. The signature of the  $p$  wave odd symmetry has to be found instead in the spectral intensities of excitations with transferred momentum  $|\mathbf{q}| \approx \pi/2$  (see Fig. 2), corresponding to a “self-nesting” of the hole pockets. This type of excitations, which lead to characteristic intensity features also in LiFeAs (see next subsection), refer to *intra-band* contributions located in a narrow momentum range similar to the conventional nesting scenario between the electron and hole pockets. In the  $s$  wave case these excitations preserve the sign of the order parameter ( $\Delta_{\mathbf{k}+\mathbf{q}} = \Delta_{-\mathbf{k}} = \Delta_{\mathbf{k}}$ ), leading to a suppression of spectral intensities in the spin DSF. In the  $p$  wave case instead, these excitations are sign reversing ( $\Delta_{\mathbf{k}+\mathbf{q}} = \Delta_{-\mathbf{k}} = -\Delta_{\mathbf{k}}$ ), with a consequent suppression in the charge DSF.

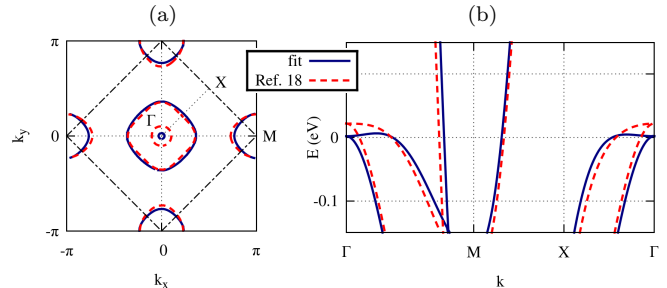


Figure 3: (color online) Fermi surface (a) and electronic dispersion (b) for the tight-binding model<sup>20</sup> (dashed line) and for the same model with hopping parameters (see Table I) fitted with the experimental Fermi surface of LiFeAs<sup>15,45</sup> (solid line).

## B. LiFeAs

While there is a general agreement about the presence of a spin-singlet  $s_{\pm}$  wave superconductivity<sup>6</sup> in other iron-based SC, where nesting dominates the low energy properties, the nature of the SC state in LiFeAs seems to be elusive. Different scenarios have been proposed in place of the  $s_{\pm}$  wave pairing, e.g., an  $s_{++}$  wave SC state, driven by the critical  $d$ -orbital fluctuations induced by moderate electron-phonon interactions<sup>46</sup>, or even a spin-triplet pairing driven by ferromagnetic fluctuations<sup>20</sup>. While the singlet pairing is supported by some neutron scattering experiments<sup>47</sup>, the unusual shape of the Fermi surface and the momentum dependency of the SC gap measured by ARPES<sup>16</sup> is in conflict with the  $s_{\pm}$  wave symmetry. Moreover, STM experiments of the QP interference<sup>48</sup> are consistent with a  $p$  wave spin-triplet state or with a singlet pairing mechanism with a more complex order parameter ( $s+id$  wave). Whereas ARPES has been proven to be powerful in measuring the momentum dependence of the SC gap on the Fermi surface<sup>15,16</sup>, it should be noted here that ARPES, since not sensitive to the order parameter phase, cannot distinguish between singlet and triplet pairing, i.e., between even ( $\Delta_{\mathbf{k}} = \Delta_{-\mathbf{k}}$ ) and odd ( $\Delta_{\mathbf{k}} = -\Delta_{-\mathbf{k}}$ ) symmetry of the order parameter. In fact, the experimental momentum dependence of the superconducting gap measured by ARPES<sup>16</sup> is consistent, in principle, with a spin-singlet as well as with a spin-triplet state, as long as the pairing mechanism correctly reproduces the gap magnitude variations along the Fermi surface.

The theoretical predictions shown in this subsection in combination with an appropriate RIXS experiment might



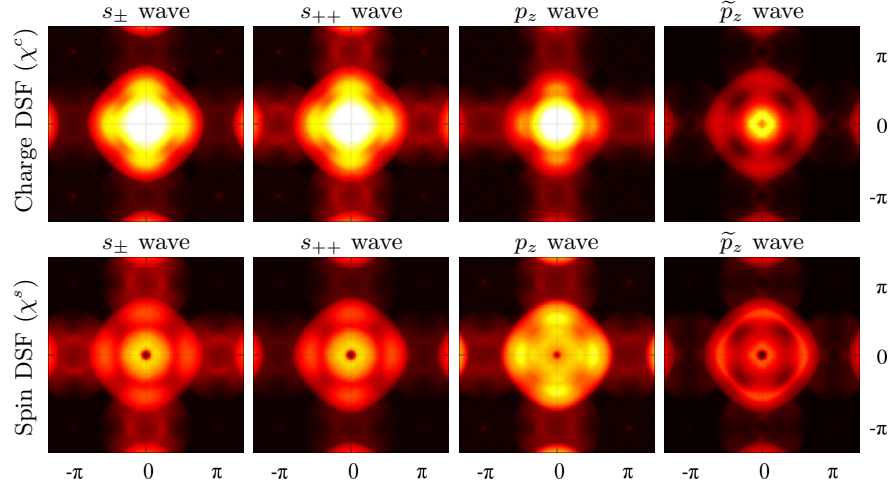


Figure 4: (color online) RIXS spectra at a fixed energy loss  $\hbar\omega = 2\Delta_0 = 12$  meV as a function of the transferred momentum  $\mathbf{q}$  for the charge and spin DSF of QP excitations in LiFeAs, calculated using Eq. (6), with the  $s_{\pm}$ ,  $s_{++}$ ,  $p_z$ , and  $\tilde{p}_z$  wave SC order parameter, summing over the contributions of the orbitals  $\alpha = yz, zx, xy$ . Spectral intensities at  $\mathbf{Q}_{AF}$  are suppressed in the charge (spin) spectra in the  $s_{\pm}$  ( $s_{++}$ ) wave state, while intensities for  $|\mathbf{q}| \approx \pi/2$  around the  $\Gamma$  point are suppressed in the charge (spin) DSF in the  $p_z$  and  $\tilde{p}_z$  ( $s_{\pm}$  and  $s_{++}$ ) state.

help to clarify this complicated and controversial situation in LiFeAs. To achieve this goal, we consider different order parameter symmetries, corresponding to spin-singlet and spin-triplet pairing. In order to properly take into account the orbital degrees of freedom of the system, we construct our model on the basis of the effective three-band tight-binding model proposed in Ref. 20, which includes the effective hoppings between the  $t_{2g}$  orbitals of the iron ions, within a single Fe-ion unit cell. Nevertheless, a comparison with ARPES measurements<sup>15,45</sup> shows that the inner hole pocket in LiFeAs is much smaller than the one produced by the tight-binding model in Ref. 20. Furthermore, the SC gap is significantly larger<sup>16</sup> on the inner hole pocket than on the outer one. For this reason, we redefine the hopping parameters in order to fit the experimental Fermi surface<sup>15,45</sup>. These parameters are given in Table I, while in Fig. 3 we compare the fitted Fermi surface (a) and bare electron dispersion (b) with the original model (cf. Ref. 20).

Besides the  $s_{\pm}$ ,  $s_{++}$ , and  $p_z$  wave defined above, we consider here also a triplet pairing order parameter  $\tilde{p}_z$ , defined as  $\Delta_{\mathbf{k}}^{\tilde{p}_z} = |\Delta_{\mathbf{k}}^{s_{\pm}}|e^{i\phi_{\mathbf{k}}}$ , i.e., having the same magnitude of the  $s_{\pm}$  (or  $s_{++}$ ) wave and the same phase  $\phi_{\mathbf{k}} = \arg \Delta_{\mathbf{k}}^{p_z}$  of the  $p_z$  wave order parameter. This SC order parameter is considered here for comparison, in order to have an example of a spin-triplet pairing which reproduces the experimental gap magnitude on the different branches of the Fermi surface in LiFeAs. Moreover, the equal gap structure in comparison to the singlet pairing models allows us to study those features of spectra which are solely attributed to the phase variation. We fix the order parameter magnitude by taking  $\Delta_0 = 6$  meV, in order to be consistent with the measured value of the SC gap in LiFeAs<sup>16</sup>. Therefore, in the case of the  $s$  wave states ( $s_{\pm}$  and  $s_{++}$ ), and of the  $\tilde{p}_z$  wave state, the gap

magnitude varies around  $\approx 4.6$  meV along the electron pockets, around  $\approx 6$  meV along the inner hole pocket, and around  $\approx 3$  meV along the outer hole pocket, with opposite sign in the case of the  $s_{\pm}$  wave symmetry, and with the phase continuously varying on the Fermi surface in the case of the  $\tilde{p}_z$  wave state. In the  $p_z$  wave case instead, the gap magnitude varies around  $\approx 4$  meV along the electron pockets, around  $\approx 0.6$  meV along the inner hole pocket, and around  $\approx 5.6$  meV along the outer hole pocket. In any of the case considered, the low energy QP excitations contribute to coherence peaks at the  $\Gamma$  point with energy in the range  $6 \text{ meV} < E < 12 \text{ meV}$  ( $\Delta_0 < E < 2\Delta_0$ ).

In Fig. 4 are shown the RIXS intensities for the charge and spin DSF at a fixed energy loss  $\hbar\omega = 2\Delta_0 = 12$  meV as a function of the transferred momentum  $\mathbf{q}$ , for different choices of the SC order parameter symmetry, calculated using Eq. (6). In LiFeAs, no nesting occurs between the hole and the electron pockets<sup>15</sup>, and therefore the peak at  $\mathbf{Q}_{AF}$  in the QP spectra, which corresponds to the scattering between hole and electron pockets, is much weaker and broader than in the LaOFeAs case. The intensive square-like intensity distribution around the center of the Brillouin zone obtained for all assumed types of pairing is a typical feature of the low energy spectrum in LiFeAs arising from interband scattering processes between the two hole-like Fermi surface sheets<sup>48,49</sup>. Indeed, as in the previous case, RIXS spectra in LiFeAs are strongly sensitive to the symmetry of the SC order parameter and on its relative phase differences along the Fermi surface. In fact, spectral intensities at  $\mathbf{Q}_{AF}$  are further suppressed in the charge and in the spin DSF respectively in the  $s_{\pm}$  wave and in the  $s_{++}$  wave SC states. This is because  $\Delta_{\mathbf{k}+\mathbf{Q}_{AF}} = \pm\Delta_{\mathbf{k}}$ , with the  $\pm$  sign corresponding to the  $s_{++}$  and  $s_{\pm}$  wave, resulting in sign preserving and sign

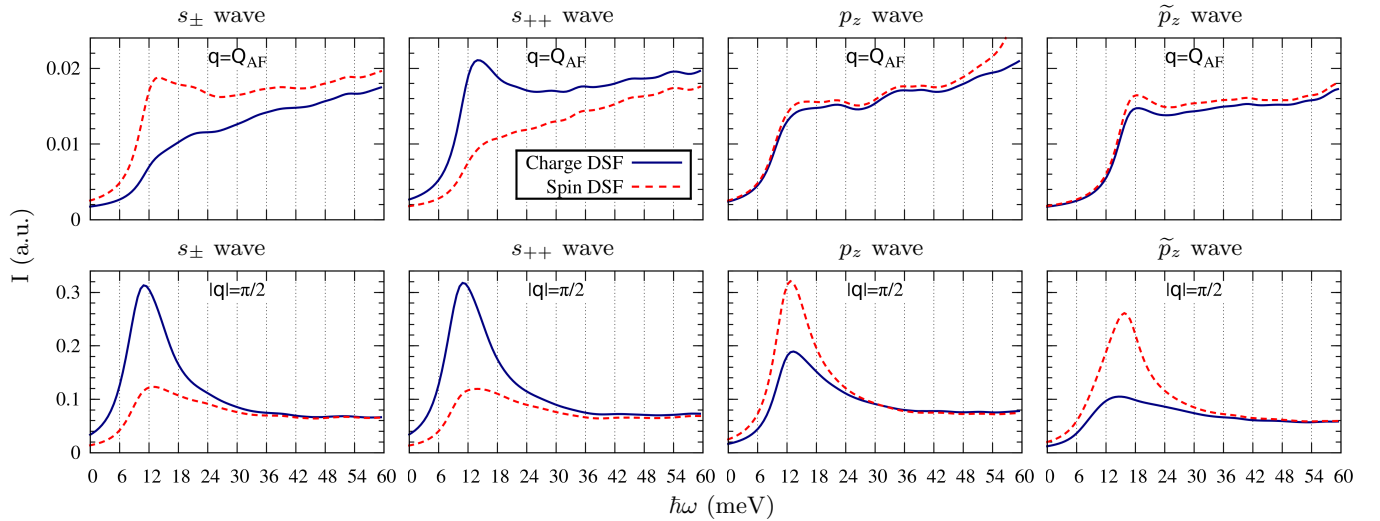


Figure 5: (color online) RIXS spectra at  $\mathbf{Q}_{AF}$  and at  $|\mathbf{q}| = \pi/2$  as a function of the energy loss for the charge (solid line) and spin (dashed line) DSF of QP excitations in LiFeAs, calculated using Eq. (6), with  $s_{\pm}$ ,  $s_{++}$ ,  $p_z$ , and  $\tilde{p}_z$  wave SC order parameter ( $\Delta_0 = 6$  meV). Spectral intensities at  $\mathbf{Q}_{AF}$  are larger for the spin (charge) DSF spectra in the  $s_{\pm}$  ( $s_{++}$ ) wave state, while intensities at  $|\mathbf{q}| = \pi/2$  around the  $\Gamma$  point are larger in the spin (charge) DSF in the  $p_z$  and  $\tilde{p}_z$  ( $s_{\pm}$  and  $s_{++}$ ) state. The intensity are in arbitrary units, chosen such that the coherence peak at  $\Gamma$  (not shown) has unitary intensity.

reversing excitations respectively. In the  $p$  wave states no suppression occur, being  $\Delta_{\mathbf{k}+\mathbf{Q}_{AF}} = \Delta_{\mathbf{k}}^*$ , i.e., with a phase difference given by  $2\phi_{\mathbf{k}}$ , resulting in charge and spin coherence factors [see Eq. (7)] which continuously vary on the Fermi surface. Again, the signature of the  $p$  wave odd symmetry is in the spectral intensities of excitations with transferred momentum  $|\mathbf{q}| \approx \pi/2$  around the  $\Gamma$  point, corresponding to a self-nesting of the larger hole pocket (see Fig. 4). While in the  $s$  wave case excitations at  $|\mathbf{q}| = \pi/2$  are sign preserving, with a consequent suppression of spectral intensities in the spin DSF, in the  $p$  wave case they are sign reversing, resulting instead in an enhancement in the spin DSF.

In order to present in the most clear way how to distinguish between the different pairing scenarios in LiFeAs, we show in Fig. 5 the RIXS spectra as a function of the energy loss for the charge and spin DSF of QP excitations at  $\mathbf{Q}_{AF}$  and at  $|\mathbf{q}| = \pi/2$ , again for different choices of the SC order parameter symmetry. As we have seen, these particular momenta are those where the sensitivity to the order parameter phase is more pronounced. In particular, spectral intensities corresponding to the transferred momentum  $\mathbf{Q}_{AF}$  are sensitive to sign changes of the order parameter between hole and electron pockets. Indeed, as one can see in Fig. 5, the charge (spin) DSF is suppressed in the  $s_{\pm}$  ( $s_{++}$ ) wave state. Therefore, a comparison between spin and charge DSF can be revealing of a sign reversal in the order parameter between disconnected branches of the Fermi surface. On the other hand, the spectral contributions of the intraband scattering within the hole pockets, which correspond to a transferred momentum  $|\mathbf{q}| \approx \pi/2$ , are strongly affected by the parity of the order parameter, and therefore can discriminate be-

tween spin-singlet (e.g.,  $s$  wave) and spin-triplet pairing (e.g.,  $p$  wave). In fact, spectral intensities at  $|\mathbf{q}| = \pi/2$  in Fig. 5 are suppressed in the spin and charge DSF respectively in the spin-singlet ( $s_{\pm}$  and  $s_{++}$  wave) and in the spin-triplet ( $p_z$  and  $\tilde{p}_z$  wave) cases. It should be noticed here that this result is general, and does not depend on the gap magnitude dependence along the Fermi surface, but only on its phase variations, and therefore is a mere consequence of the odd parity of the order parameter. This aspect is clearly displayed by the two panels of Fig. 5 referring to the  $p$  wave state at  $|\mathbf{q}| = \pi/2$ . The suppression of the charge DSF occurs for both  $p_z$  and  $\tilde{p}_z$  wave, which have a different gap magnitude dependence, but nevertheless the same phase variations and the same parity.

#### IV. CONCLUSIONS

We have shown that RIXS spectra of quasiparticle excitations are sensitive to phase differences of the SC order parameter along the Fermi surface, and hence allow one to distinguish among different SC states, in particular between spin-singlet and spin-triplet pairing and between sign preserving and sign reversing  $s$  wave states in iron-based superconductors. In particular, RIXS spectral intensities corresponding to a self-nesting of the hole pockets can discriminate between singlet and triplet pairing, while RIXS spectra corresponding to a scattering between hole and electron pockets [ $\mathbf{Q}_{AF} = (\pi, 0)$ ] can discriminate between a  $s_{\pm}$  wave and a  $s_{++}$  wave order parameter.

- <sup>1</sup> A. J. Leggett, *Nature Phys.* **2**, 134 (2006).
- <sup>2</sup> J. R. Kirtley, C. C. Tsuei, J. Z. Sun, C. C. Chi, L. S. Yu-Jahnes, A. Gupta, M. Rupp, and M. B. Ketchen, *Nature* **373**, 225 (1995).
- <sup>3</sup> C. C. Tsuei, J. R. Kirtley, Z. F. Ren, J. H. Wang, H. Raffy, and Z. Z. Li, *Nature* **387**, 481 (1997).
- <sup>4</sup> A. Damascelli, Z. Hussain, and Z.-X. Shen, *Rev. Mod. Phys.* **75**, 473 (2003).
- <sup>5</sup> K. Kuroki and R. Arita, *Phys. Rev. B* **64**, 024501 (2001).
- <sup>6</sup> I. I. Mazin, D. J. Singh, M. D. Johannes, and M. H. Du, *Phys. Rev. Lett.* **101**, 057003 (2008).
- <sup>7</sup> K. Kuroki, S. Onari, R. Arita, H. Usui, Y. Tanaka, H. Kontani, and H. Aoki, *Phys. Rev. Lett.* **101**, 087004 (2008).
- <sup>8</sup> C. C. Tsuei and J. R. Kirtley, *Rev. Mod. Phys.* **72**, 969 (2000).
- <sup>9</sup> C.-T. Chen, C. C. Tsuei, M. B. Ketchen, Z.-A. Ren, and Z. X. Zhao, *Nature Phys.* **6**, 260 (2010).
- <sup>10</sup> J. E. Hoffman, K. McElroy, D.-H. Lee, K. M. Lang, H. Eisaki, S. Uchida, and J. C. Davis, *Science* **297**, 1148 (2002).
- <sup>11</sup> K. McElroy, R. Simmonds, J. Hoffman, D. Lee, J. Orenstein, H. Eisaki, S. Uchida, and J. Davis, *Nature* **422**, 592 (2003).
- <sup>12</sup> T. Hanaguri, Y. Kohsaka, J. C. Davis, C. Lupien, I. Yamada, M. Azuma, M. Takano, K. Ohishi, M. Ono, and H. Takagi, *Nature Physics* **3**, 865 (2007).
- <sup>13</sup> Y. Kohsaka, C. Taylor, P. Wahl, A. Schmidt, J. Lee, K. Fujita, J. W. Alldredge, K. McElroy, J. Lee, H. Eisaki, S. Uchida, D. H. Lee, and J. C. Davis, *Nature* **454**, 1072 (2008).
- <sup>14</sup> T. Hanaguri, Y. Kohsaka, M. Ono, M. Maltseva, P. Coleman, I. Yamada, M. Azuma, M. Takano, K. Ohishi, and H. Takagi, *Science* **323**, 923 (2009).
- <sup>15</sup> S. V. Borisenko, V. B. Zabolotnyy, D. V. Evtushinsky, T. K. Kim, I. V. Morozov, A. N. Yaresko, A. A. Kordyuk, G. Behr, A. Vasiliev, R. Follath, and B. Büchner, *Phys. Rev. Lett.* **105**, 067002 (2010).
- <sup>16</sup> S. V. Borisenko, V. B. Zabolotnyy, A. A. Kordyuk, D. V. Evtushinsky, T. K. Kim, I. V. Morozov, R. Follath, and B. Büchner, *Symmetry* **4**, 251 (2012).
- <sup>17</sup> C. Platt, R. Thomale, and W. Hanke, *Phys. Rev. B* **84**, 235121 (2011).
- <sup>18</sup> Y. Wang, A. Kreisel, V. B. Zabolotnyy, S. V. Borisenko, B. Büchner, T. A. Maier, P. J. Hirschfeld, and D. J. Scalapino, *Phys. Rev. B* **88**, 174516 (2013).
- <sup>19</sup> F. Ahn, I. Eremin, J. Knolle, V. B. Zabolotnyy, S. V. Borisenko, B. Büchner, and A. V. Chubukov, *Phys. Rev. B* **89**, 144513 (2014).
- <sup>20</sup> P. M. R. Brydon, M. Daghofer, C. Timm, and J. van den Brink, *Phys. Rev. B* **83**, 060501 (2011).
- <sup>21</sup> M. Tinkham, *Introduction to Superconductivity* (Dover Publications, Mineola, New York, 2004).
- <sup>22</sup> T. Hanaguri, S. Niitaka, K. Kuroki, and H. Takagi, *Science* **328**, 474 (2010).
- <sup>23</sup> T. Hanaguri, S. Niitaka, K. Kuroki, and H. Takagi, (2010).
- <sup>24</sup> S. Sykora and P. Coleman, *Phys. Rev. B* **84**, 054501 (2011).
- <sup>25</sup> P. Marra, S. Sykora, K. Wohlfeld, and J. van den Brink, *Phys. Rev. Lett.* **110**, 117005 (2013).
- <sup>26</sup> L. Braicovich, L. J. P. Ament, V. Bisogni, F. Forte, C. Aruta, G. Balestrino, N. B. Brookes, G. M. De Luca, P. G. Medaglia, F. Miletto Granozio, M. Radovic, M. Salluzzo, J. van den Brink, and G. Ghiringhelli, *Phys. Rev. Lett.* **102**, 167401 (2009).
- <sup>27</sup> C. Ulrich, L. J. P. Ament, G. Ghiringhelli, L. Braicovich, M. Moretti Sala, N. Pezzotta, T. Schmitt, G. Khaliullin, J. van den Brink, H. Roth, T. Lorenz, and B. Keimer, *Phys. Rev. Lett.* **103**, 107205 (2009).
- <sup>28</sup> H. Yavaş, M. van Veenendaal, J. van den Brink, L. J. P. Ament, A. Alatas, B. M. Leu, M.-O. Apostu, N. Wizen, G. Behr, W. Sturhahn, H. Sinn, and E. E. Alp, *Journal of Physics: Condensed Matter* **22**, 485601 (2010).
- <sup>29</sup> L. J. P. Ament, M. van Veenendaal, T. P. Devereaux, J. P. Hill, and J. van den Brink, *Rev. Mod. Phys.* **83**, 705 (2011).
- <sup>30</sup> L. J. P. Ament, G. Ghiringhelli, M. Moretti Sala, L. Braicovich, and J. van den Brink, *Phys. Rev. Lett.* **103**, 117003 (2009).
- <sup>31</sup> E. Kaneshita, K. Tsutsui, and T. Tohyama, *Phys. Rev. B* **84**, 020511 (2011).
- <sup>32</sup> K.-J. Zhou, Y.-B. Huang, C. Monney, X. Dai, V. N. Strocov, N.-L. Wang, Z.-G. Chen, C. Zhang, P. Dai, L. Patthey, J. van den Brink, H. Ding, and T. Schmitt, *Nat Commun* **4**, 1470 (2013).
- <sup>33</sup> L. W. Harriger, H. Q. Luo, M. S. Liu, C. Frost, J. P. Hu, M. R. Norman, and P. Dai, *Phys. Rev. B* **84**, 054544 (2011).
- <sup>34</sup> L. Braicovich, J. van den Brink, V. Bisogni, M. M. Sala, L. J. P. Ament, N. B. Brookes, G. M. De Luca, M. Salluzzo, T. Schmitt, V. N. Strocov, and G. Ghiringhelli, *Phys. Rev. Lett.* **104**, 077002 (2010).
- <sup>35</sup> M. Le Tacon, G. Ghiringhelli, J. Chaloupka, M. M. Sala, V. Hinkov, M. W. Haverkort, M. Minola, M. Bakr, K. J. Zhou, S. Blanco-Canosa, C. Monney, Y. T. Song, G. L. Sun, C. T. Lin, G. M. De Luca, M. Salluzzo, G. Khaliullin, T. Schmitt, L. Braicovich, and B. Keimer, *Nat Phys* **7**, 725 (2011).
- <sup>36</sup> M. P. M. Dean, G. Dellea, R. S. Springell, F. Yakhou-Harris, K. Kummer, N. B. Brookes, X. Liu, Y.-J. Sun, J. Strle, T. Schmitt, L. Braicovich, G. Ghiringhelli, I. Božović, and J. P. Hill, *Nat. Mater.* **12**, 1019 (2013), letter.
- <sup>37</sup> M. W. Haverkort, *Phys. Rev. Lett.* **105**, 167404 (2010).
- <sup>38</sup> P. Marra, K. Wohlfeld, and J. van den Brink, *Phys. Rev. Lett.* **109**, 117401 (2012).
- <sup>39</sup> B. M. Andersen and P. Hedegård, *Phys. Rev. Lett.* **95**, 037002 (2005).
- <sup>40</sup> M. Sigrist, *AIP Conference Proceedings* **789**, 165 (2005).
- <sup>41</sup> S. Raghu, X.-L. Qi, C.-X. Liu, D. J. Scalapino, and S.-C. Zhang, *Phys. Rev. B* **77**, 220503 (2008).
- <sup>42</sup> H.-Y. Kee and C. M. Varma, *Phys. Rev. B* **58**, 15035 (1998).
- <sup>43</sup> H.-Y. Kee and Y. B. Kim, *Phys. Rev. B* **59**, 4470 (1999).
- <sup>44</sup> K.-K. Voo, W. C. Wu, J.-X. Li, and T. K. Lee, *Phys. Rev. B* **61**, 9095 (2000).
- <sup>45</sup> J. Knolle, V. B. Zabolotnyy, I. Eremin, S. V. Borisenko, N. Qureshi, M. Braden, D. V. Evtushinsky, T. K. Kim, A. A. Kordyuk, S. Sykora, C. Hess, I. V. Morozov, S. Wurmehl, R. Moessner, and B. Büchner, *Phys. Rev. B* **86**, 174519 (2012).
- <sup>46</sup> H. Kontani and S. Onari, *Phys. Rev. Lett.* **104**, 157001 (2010).



- <sup>47</sup> A. E. Taylor, M. J. Pitcher, R. A. Ewings, T. G. Perring, S. J. Clarke, and A. T. Boothroyd, Phys. Rev. B **83**, 220514 (2011).
- <sup>48</sup> T. Hänke, S. Sykora, R. Schlegel, D. Baumann, L. Harnagea, S. Wurmehl, M. Daghofer, B. Büchner, J. van den Brink, and C. Hess, Phys. Rev. Lett. **108**, 127001 (2012).
- <sup>49</sup> C. Hess, S. Sykora, T. Hänke, R. Schlegel, D. Baumann, V. B. Zabolotnyy, L. Harnagea, S. Wurmehl, J. van den Brink, and B. Büchner, Phys. Rev. Lett. **110**, 017006 (2013).